

Soil Erosion Modeling For Managing Natural Hazards with Determining Four adequate Cell Size Factor of Slope Length

Mohammad Almasinia^{1*}, Hasan Alizadeh Saloomahaleh²

1- Department of Geography, Payame Noor University, PO BOX 19395-3697 Tehran, Iran.

2- Department of Geology, Payame Noor University, PO BOX 19395-3697 Tehran, Iran.

* Corresponding Author: almasinia78@gmail.com

Received: 21 September, 2017 / Accepted: 01 March 2018 / Published online: 03 March 2018

Abstract

Soil loss erosion is one of the most serious environmental problems (widespread globally), which is a menace to sustainable ecosystems and agriculture. As the previous studies show, the world's highest soil loss rates due to erosion are in three continents, i.e. Asia, Africa, and South America. A new method was proposed to statistically evaluate the most appropriate cell size for LS factor input and to study the effects of using the appropriate cell size in calculating the erosion's total soil loss. Different models have been used. Among others, Revised Universal Soil Loss Equation (RUSLE) is used in this study. This model needs five parameters such as slope length and steepness (LS), crop cover (C), rainfall erosivity (R), soil erodability (K), and prevention practice (P) with the help of Geographical Information System (GIS) using raster technique whereby all the parameters are mapped in the form of grid layers of a specific cell size. The proposed methodology shows a way to comprehend how to implement and estimate annual soil loss erosion. Different cell sizes are selected and applied to data of Nibong Tebal Penang as a sample test. LS factors have been comprised where semivariogram models are fitted to the height information based on the 20-m contourline topographic map. The results show that with increasing cell size up to 50m, the nugget effect decreases and spatial dependency increases. The best spatial dependency and high variances and diversity of 50 m cell spacing, the Digital Elevation Model (DEM) of this cell size is found the most appropriate for such dataset. According to the results, by using geostatistical techniques which can identify the best DEM cell size in order to make the suitable raster analysis for decision in the case of DEM spacing, could be applied to select a suitable cell spacing in DEM to predict topographical factor in soil erosion modeling. Basically, these techniques lead to find DEMs 50m from topographic map with 20m interval contour lines. In general, the results of this study have confirmed that the geostatistical analysis and statistical approaches together can be applied to select an adequate cell spacing in DEM and also to predict topographical factor in RUSLE model.

Keywords: Environmental problems; Soil erosion; GIS; (Nibong Tebal Penang, North West of Malaysia).

1- Introduction

Soil erosion is one of the significant environmental hazard and land degradation challenge experienced worldwide. About 80% of the world's agricultural land suffer from moderate to severe erosion (Moses, 2017). Soil

erosion is broadly defined as the accelerated removal of topsoil from the land surface through water, wind or tillage (FAO, 2016). One of the main causes of soil erosion is water erosion, which is the loss of topsoil due to water (Jim

Ritter, 2015). Water erosion on agricultural land occurs mainly when overland flow entrains soil particles detached by drop impact or runoff, often leading to clearly defined channels such as rills or gullies. Wind erosion occurs when dry, loose, bare soil is subjected to strong winds. Wind erosion is common in semiarid areas where strong winds can easily mobilize soil particles, especially during dry spells. This dynamic physical aeolian process includes the detachment of particles from the soil, transport for varying distances depending on site, particle and wind characteristics, and subsequent deposition in a new location, causing onsite and offsite effects (FAO, 2016). Ritter, (2015) emphasized that Raindrops fall directly on topsoil. The impact of the raindrops loosens the material bonding it together, allowing small fragments to detach. If the rainfall continues, water gathers on the ground, causing water flow on the land surface, known as surface water runoff. This runoff carries the detached soil materials away and deposits them elsewhere.

The FAO estimates that 11.6% of Africa north of the Equator, and 17.1% of the Near East, is subject to water erosion, as are 90 million hectares (of a total of 297 million) in India and Malaysia. In Nepal the removal of topsoil by the monsoon rains do double harm, first by denuding the hillsides, and second by filling the Himalayan rivers with silt. Therefore, As the previous studies show, the world's highest soil loss rates due to erosion are in three continents, i.e. Africa, South America, and Asia (south east of Asia in Malaysia) specially in the study area, averaging approximately 26,768 pounds (12.1 metric tons) to 35,637 pounds (16.2 metric tons) for all them.

In recent decades, several models have been developed for estimating soil erosion by some other researchers such as Universal Soil Loss Equation (USLE) (Wischmayer and Smith, 1965), Modified 2 Universal Soil Loss Equation (MUSLE) (Williams, 1975), and Revised Universal Soil Loss Equation (RUSLE) (Renard

et al., 1997), Water Erosion Prediction Project (WEPP) (Flanagan and Livingston, 1995) and so on. Gelagay, (2016) attempted to assess and map the spatial distribution of sediment yield of Koga watershed in a GIS and remote sensing environment. Turner *et al.* (2018) documented that all of the cases of soil erosion in Colorado, Kansas, Nebraska, North Dakota, and Texas reduced watershed capacities to regulate runoff occurred in areas where recent land use has shifted away from native and towards increased cultivated landscapes wind erosion.

Previous twenty year process has been exhibited which agree with the using GIS tools propagate together USLE and RUSLE- emerged justification of the algorithm applied to raise the slope length (Kay *et al.*, 2016; Merritt *et al.*, 2003; Tung *et al.*, 2018). Geographic Information System (GIS) and Remote Sensing (RS) integrations can recognize soil erosion areas in which there exists some potential risk of extensive soil erosion and the estimated amount of soil loss on various locations. Today, soil erosion is a more ominous than any other time in history. Soil loss and its associated impacts are one of the most important (yet probably the least well-known) environmental problems of today's life. There is no more destructive phenomenon than those caused by wind and water on a global scale. The soil erosion factors, e.g. water, wind, and tillage, affect both the agriculture and the natural environment. Numerous models of various prediction capabilities and utilities have been developed. The advent of technological tools such as RS and GIS has significantly enhanced the usefulness of soil erosion models. The coupling of GIS and RS with empirical and process-based soil erosion models have improved their predictive capability. GIS stores the essential database needed as input for modeling erosion and elaboration of maps of erosion-affected areas. RS and GIS tools also allow the scaling up of the modeled data from

small plots (e.g. RUSLE) for large areas (Humberto Blanco *et al.*, 2015).

Currently, the data from RUSLE model are readily available in GIS format. The GIS capabilities are the unique representation of erosion characteristics within a grid cell environment at fine resolutions. The accuracy of RUSLE calculations using larger grid sizes can be studied within the GIS environment by applying the equation at a wide range of cell sizes. This type of erosion is triggered by anthropogenic causes such as deforestation, slash and burn agriculture, intensive plowing, intensive and uncontrolled grazing, and biomass burning (Terrence *et al.*, 2002). In RUSLE, the LS factor is much more essential to the soil erosion. The soil erosion increases as the slope length and steepness increase, although it is more sensitive to slope steepness than to slope length. Therefore, the LS factor is combined from two factors as follows:

The slope length factor L which is a fundamental slope length measured in meters.

Considering the importance of soil erosion is to identify, anticipate and prevent the effective factors. So, topography factor is the main factor in RUSLE method. The LS factor depends on the slope length and steepness, and shows topographic effects on soil loss. This factor is calculated using DEM. DEM is used to select the most appropriate cell size for calculating LS. In such cases, it is very frequent that the correct cell size is not given enough attention so that this ignorance will be inherited into the subsequent use of the raster layer, e.g. calculating the total annual soil loss.

The RUSLE has been used in this context efficiently to model the soil erosion. The spatial parameters in RUSLE equation, i.e. topography and land use can be generated by remote sensing techniques. These factors can be converted to raster layers as the input layer into a GIS for analysis and provide a soil erosion risk map. There are different factors in the soil

erosion but water and wind are most important than them. In Malaysia peninsular, the water erosion is the most significant factor due to high mean annual rainfall, storm density and frequency (Ooshaksaraie *et al.*, 2009). Also the most significant effect is observed when the vegetation is disturbed or removed. The removal of vegetation leads to an increase in the speed and volume of surface runoff. So, the increasing of the volume and velocity of the surface runoff (especially in the hilly terrains) causes it to be considered in soil erosion. The erosion by running water may take place in the form of rill or gully erosion notably in the loose sandy granitic soils or reworked residual soils (University of Malaya Consultancy Unit, 2003). Malaysia is subjected to high intensity and more frequent rain storms than most developed countries and thus it requires more stringent control measures, structural or non-structural to deal with the problem (Ooshaksaraie *et al.*, 2009).

In Malaysia, several soil erosion studies have been conducted using previous approach (USLE): including the soil erosion study of the Bakun Dam project (Samad and Patah, 1997), the soil erosion risk assessment for Genting Highlands (Jusoff and Chew, 1998), and the soil erosion and soil risk maps for Langkawi Island (Wan Yusof and Baban, 1999). The deterministic and rigid decision approach is a common use of GIS for formulation assessment. This method is based on two assumptions: first, the data set is complete and free of errors and second, the decision rule does not add any error to the outcome. However, it is clear that geographically based data set without error does not exist due to measurement error.

Generally, the soil erosion takes place in two different kinds of process. First, detaching the individual particles of the soil mass, and second, transporting their erosive factors, e.g. running wind and water. When there not exists enough energy to transfer sediment particles, sedimentation will occur. There are two main

types of erosion: geologic (natural) and accelerated erosion. The erosion is a natural process which can level mountain ranges over millions of years. New soils can be formed through the slow weathering of the parent rock material and from the deposition of airborne or waterborne sediments. Under the normal climatic conditions and with natural ground cover, the soil erosion can often balance out with the rate of soil production. This is called natural or geological erosion.

Erosion can be accelerated by human activities. The removal of surface vegetation and residue cover occurs in:

- Agricultural Cultivation
- Rangeland Grazing
- Forest Harvesting
- Surface Mining
- Urban Highway Construction

All these activities disturb the soil structure and reduce the soil's resistance for detaching. RUSLE is a series of mathematical equations that estimates the average annual soil loss and sediment yield resulting from in terrill and rill erosion. RUSLE is an exceptionally well-validated and documented equation. RUSLE is a model to predict annual soil loss erosion at longtime average, based on several parameters, i.e. slope length and steepness, rainfall-runoff, cover management, soil erodibility and support practice. The yield of slope length (L) and steepness (S) is topographic factor LS, implying the topographic effect on soil loss.

For an accurate prediction, obtaining the spatial dependency with an appropriate DEM spacing, which represents the spatial characteristics in the LS factor, is essential. It is clear that choosing appropriate DEM spacing is very important and may affect the results of consequent computation such as soil loss (due to erosion). A new method proposed the objectives to statistically evaluate the most appropriate cell

size for LS factor input and to study the effects of using the appropriate cell size in calculating the erosion's total soil loss.

2- Study Area and Datasets

The study area Nibong Tebal Penang in which the northwest region of peninsular Malaysia is located between latitude $5^{\circ} 09' 57.1''$ N and logtitude $100^{\circ} 28' 40.5''$ E as indicated in Figure 1. The climate in this area is influenced by both the northeast and southwest monsoons and annual rainfall is approximately 1300mm in the lower plain, but more in the hilly and mountainous area. Maximum rainfall occurs during September to January and Temperature is usually 27°C , Wind NW at 0 km/h, 87% Humidity (Malaysian Meteorology Department, 2018). The extent of this area is approximately 110 Km², 90 % of which is covered by forests.

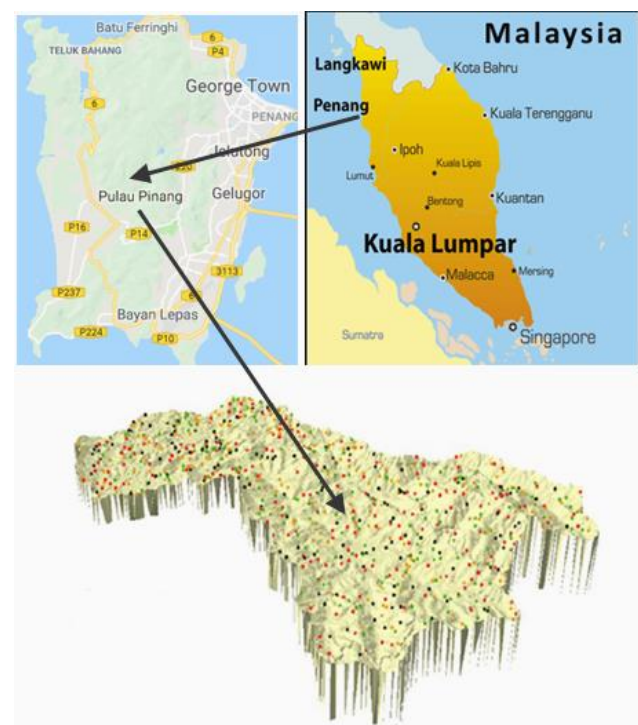


Figure 1) The study area .

Data needed for this research include:

- R factor (from rainfall data)
- K factor (obtained from soil map and soil samples)

- LS factor (obtained from topographic map- contours)
- C factor (obtained from the Remote Sensing image)
- P factor (obtained from Remote Sensing image and previous site visit)

Data that contain maps of land use type acquired from Department of Town Regional Planning and the soil maps with the P, C, and K

factors obtained from the Agriculture Department. Moreover, the digital topographic map and its derivative LS factor can be gained from the Survey and Mapping Department (JUPEM). Finally, rainfall data and R factor were obtained from information recorded in the Meteorological Department, Malaysia. As shown the study area and the captured data in Figure 2.

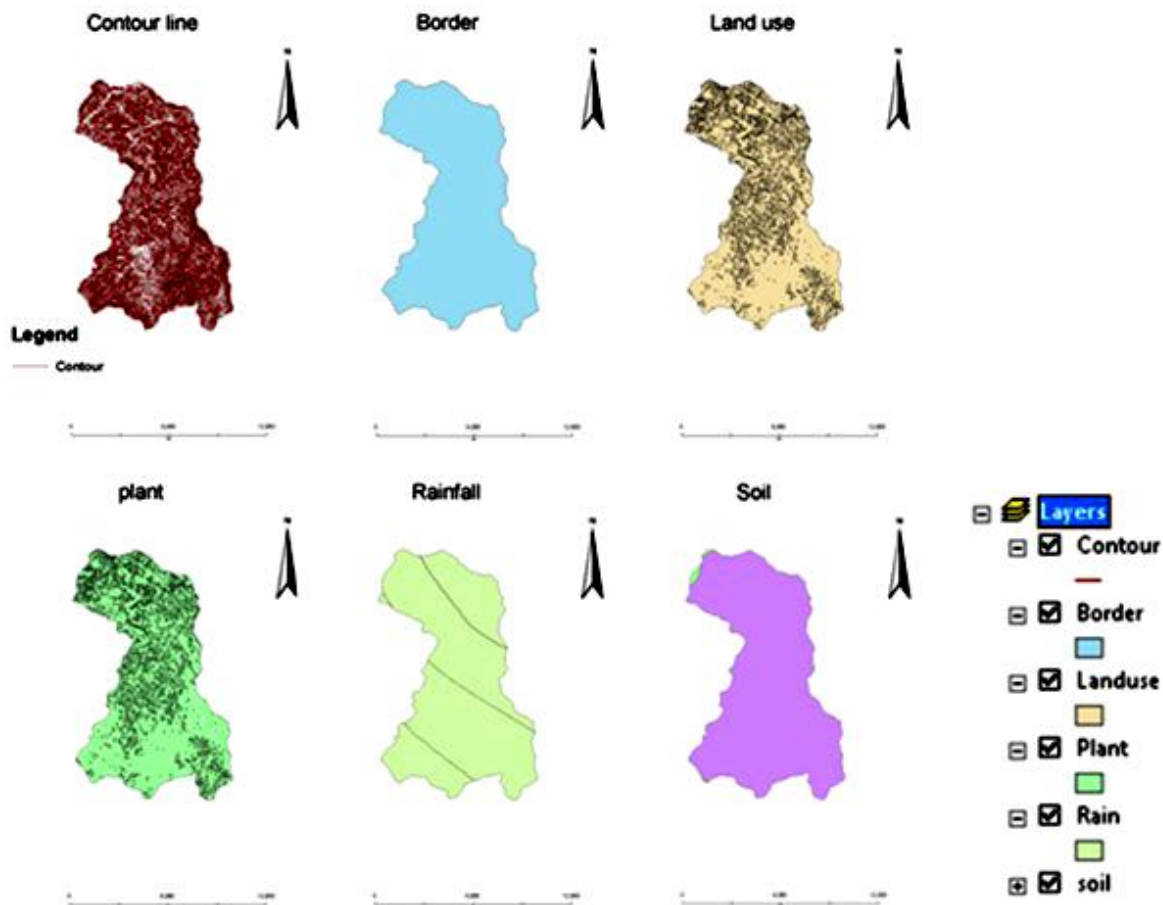


Figure 2) The study area and required data for RUSLE model.

3- Methodology

The framework of the methodology is based on three steps, i.e. capturing data, processing and analyzing of DEM for obtaining the appropriate cell size, and concluding and providing annual soil erosion map, which would help to figure out all desired parameters. Collections of hydrological and topographic maps, satellite

images, and soil samples statistical analysis via mapping of annual soil loss erosion with five factors implemented to achieve the aim of the research.

The factors calculate the effect of slope steepness (S) and slope length (L) on erosion. The slope steepness and slope length factor had been calibrated from a digitized topographic map of the study area. The digitized topographic map in line format (GIS shapefile) was then converted to digital elevation model (DEM) using TIN to grid extension.

$E = 9.28 - 8838.15$ (Eq. 1)
 Where, P= Average annual rainfall in mm, R computed from the relation the Eq 2:

$R = EI30/ 1000$ (Eq. 2)
 Where, EI30 = annual summation of rainfall energy in 30-minute intensity (suggested 75 mm/hr).

Table 1) The average rainfall in the study area.

FID	Shape	ID	GRIDCODE	ALUE	COUNT	LABLE	AVGRAIN
0	Polygon	1	4	4	668924	1349-1420	1385
1	Polygon	2	3	3	735428	1279-1349	1314
2	Polygon	3	2	2	1092996	1210-1279	1245
3	Polygon	3	2	2	1092996	1210-1280	1245
4	Polygon	4	1	1	1405308	1140-1210	1175

The generated data from above equation were entered into an ArcGIS database for spatial distribution analysis of rainfall erosivity around the study area. Table 1 shows classified data

into four groups including 1385, 1314, 1245 and 1175. Figure 3 shows the process to provide R factor.

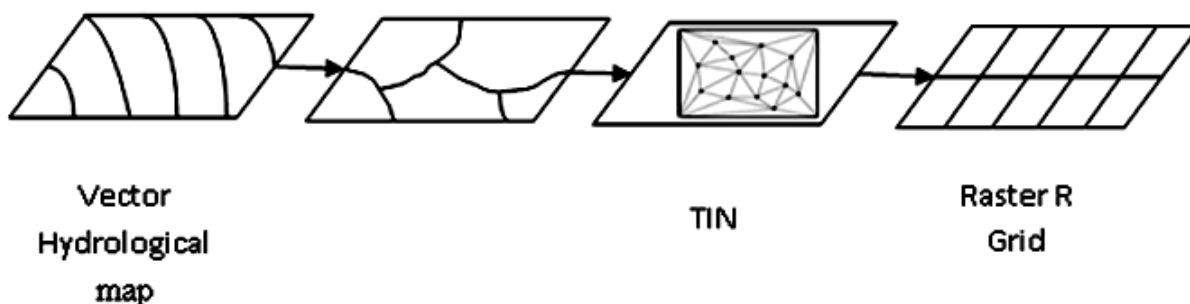


Figure 3) The process to generate R factor.

Based on contour line with 20m interval TIN generated and boundary. TIN layer converts into a raster layer based on four cell sizes comprise 30, 50, 100 and 300 m resolution to create the most appropriate celsize. Figure 4 shows the distribution of rainfall in different parts of the study area.

In this study, the soil erodibility equation and nomograph modified by Wischemier and Smith (1978) had been applied to quantify soil erodibility factor.

The soil erodability factor was calculated from the data obtained from grain size analysis, structure, permeability, and organic matter content by the Eq. 3:

$$K = [2.1 \times 10^{-4} (12 - O.M \%) (N1 \times N2)1.14 + 3.25 (S - 2) + 2.5 (P - 3)] / 100 \quad \text{(Eq. 3)}$$

Soil classification of the study area is divided into two types of soil with different soil characteristics. Table 2 shows the detail of soil types.

Table 2) K values for different soil texture.

Type soil	Permeability (%)	Silt (%)	Sand (%)	Fine sand (%)	Permeability/ Silt+ sand (%)	Organic materials (%)	K values (%)
Rengam	19.80	5.80	27.80	46.6	0.59	2.80	0.26
Serdang	18.00	4.30	41.3	36.4	0.39	5.24	0.18

In equation RUSLE, land cover is very important for the calculation, as well as soil loss which depend on the sensitivity to vegetation cover with slope steepness and length factor (Renard and Ferreira, 1993; Benkobi *et al.*,

1994; Biesemans *et al.*, 2000). Vegetation cover is an essential factor for protection of soil that causes to dissipate the raindrop energy before reaching the soil surface. Index value of crop management factor was estimated by using

vegetation characteristics derived from satellite images. Crop cover index is obtained by referring to theory of Morgan (1986) for each type of crop management in the study area.

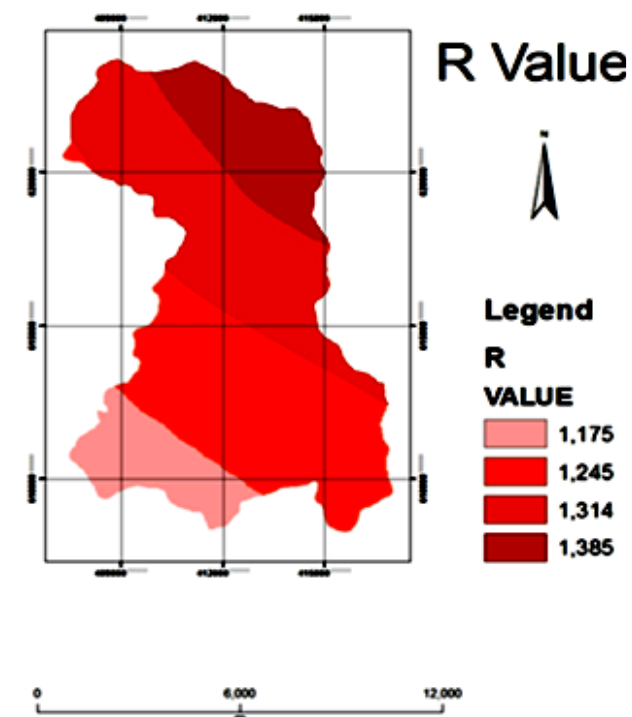


Figure 4) The distribution of rainfall in different parts of the study area

Table 3) Classification of C factors

Landuse type	C value
Water Bodies	0.000
Dense Forest	0.001
Forest	0.002
Orchard	0.1
Open Space	0.3

Table 3 indicates more than 90 percent of the study areas, were covered by forest. With the

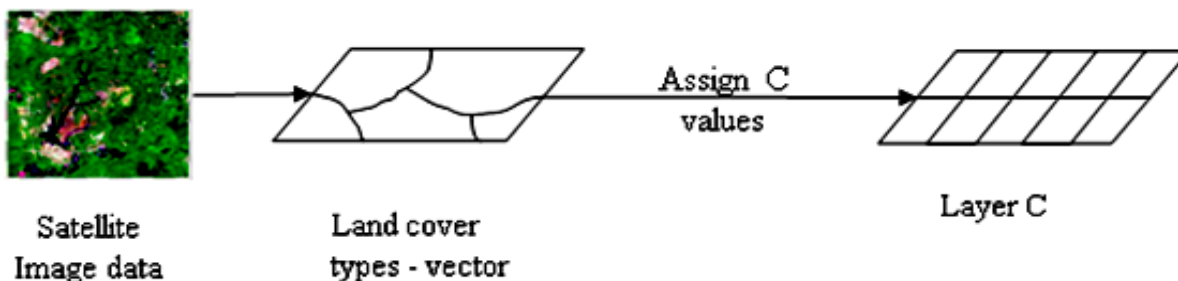


Figure 5) The process of generating C factor.

values listed in the Table 3, the grid can be generated with the C factor in study area. The result is shown in Figure 5 that shows how to capture C values.

The selected model influences the prediction of the unknown values. Kriging uses the semivariance to measure the spatially correlated component that is computed by the Eq. 4:

$$Y(h)1/2 [z(x_i) - z(x_j)]^2 \quad (\text{Eq. 4})$$

$z(x_i)$ and $z(x_i + h)$ = values of variable z at x_i and $x_i + h$, respectively.

x_i and $x_i + h$ = position in two dimensions.

Kriging is an advanced geostatistical procedure that generates an estimated surface from a scattered set of points with Z-values. Unlike the other interpolation methods supported by ArcGIS spatial analyst, kriging involves an interactive investigation of the spatial behavior of the phenomenon represented by the Z-values before selecting the best estimation method for generating the output surface.

Exploratory Spatial Data Analysis (ESDA) promotes understanding about natural phenomena so that it can make better decisions on the issue related to the data.

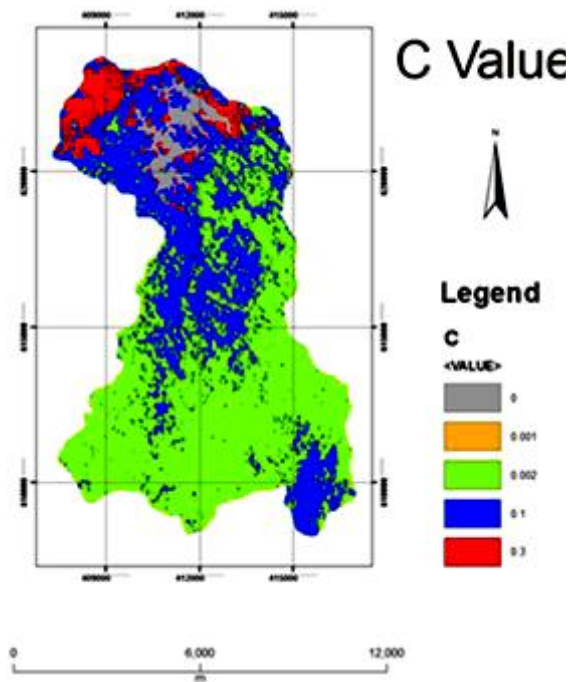


Figure 6) Map provided for the C values.

Some methods in the geostatistical analyst require that the data to be normally distributed. If data points are not normally distributed, they can be close to normal using of different transformation option. There are two methods as follows.

The Box-Cox transformation is shown by the Eq. 5:

$$Y(s) = (Z(s)^\lambda - 1)/\lambda, \text{ for } \lambda \neq 0 \quad (\text{Eq 5})$$

The log transformation is actually a special case of the Box-Cox transformation when $\lambda = 0$; the transformation is described by the Eq. 6:

$$Y(s) = \ln(Z(s)), \text{ for } Z(s) > 0 \quad (\text{Eq 6})$$

Where \ln is the natural logarithm.

The log transformation is often used where the data has a positively skewed distribution and there are a few very large values. The log transformation will help make the variances more constant and it normalizes the data if these large values are located in the study area.

The geostatistical analyst can provide various types of map layers including probability maps, quantile maps, prediction maps and prediction standard error maps. The method used in this research is the universal probability by using

spherical model because can be used to predict where values exceed a critical threshold. Calculation equation spherical is shown in the Eq. 7:

$$g(h) = \{c_0 \cdot \left(1.5(h/a) - 0.5(h/a)^3\right) \text{ if } h \leq a \quad (\text{Eq. 7})$$

Universal kriging assumes that the spatial variation in Z values has a drift or a trend in addition to the spatial correlation between the sample points. Typically, universal kriging incorporates a first order (plane surface) or a second order (quadratic surface) polynomial in the kriging process.

After fitting to the model, RMS (Root Mean Square Error) is criterion to select optimal models for skewness estimations and accuracy which is used. The Eq. 8 shown as follow:

$$\text{RMS} = \sqrt{1/n \sum_{i=1}^n (z_{i,\text{act}} - z_{i,\text{est}})^2} = \text{RMS}/S \quad (\text{Eq 8})$$

Where:

n = number of points

$z_{i,\text{act}}$ = known value of point i

$z_{i,\text{est}}$ = estimated value of point i

s = standard error.

RMSE represents the degree of accuracy which is estimated to be least for skewness. The RMS statistic is available for all exact local methods. But the standardized RMS is only available for kriging because the variance is required for the computation. The interpretation of the statistics is:

A better interpolation method should yield a smaller RMS and a standardized RMS closer to 1.

There are several methods to calculate the topography factors. The Eq. 9 is provided by Wischeier and Smith (1978). Using the kriging method to prepare relevant information for them and using statistical techniques can achieve the most appropriate digital elevation model.

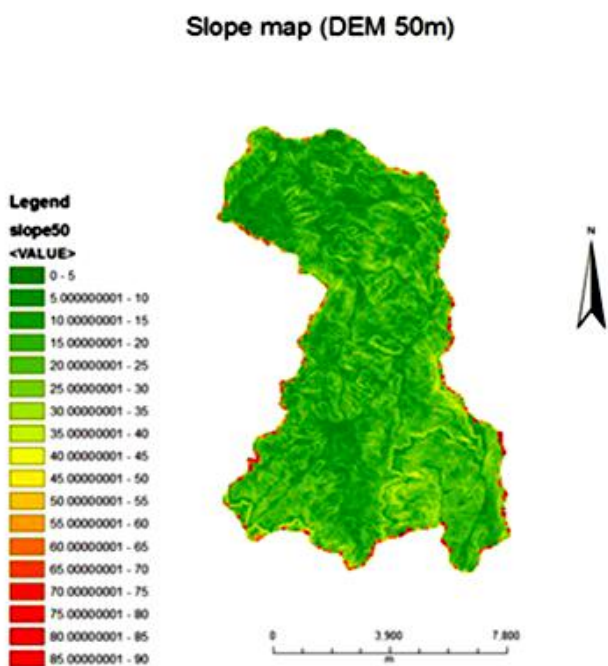


Figure 7) Slope created from DEM 50m by 50m.

$$LS = (1/22.13)n(0.065 + 0.045s + 0.0065s^2) \quad (\text{Eq. 9})$$

Where, l is the slope length (m) and s is the slope gradient in percent. $n = 0.5$ for Slope $> 5\%$, 0.4 for slope 3.5 to 4.5% , 0.3 for slope 1 to 3.5% , and 0.2 for slope less than 1 . The Eq. 11 is provided by McCool *et al.* (1989).

$$LS = (1 / 22) m (10.8 \sin b + 0.03) \quad \text{for slopes} < 9.0\%, \quad (\text{Eq. 10})$$

$$LS = (1 / 22) m (16.8 \sin b + 0.5) \quad \text{for slopes} > 9.0\% \quad m = F / (1 + F), \quad \text{and} \quad F = (\sin b / 0.0896) / (3 \sin b 8.0 + 0.56)$$

The Eq 3.12 is obtained by McCool *et al.* (1989)

$$LS = (1/ 22.13)0.5, (0.172 s - 0.55) \quad (\text{Eq. 11})$$

Where:

l = slope length in meters, and s = slope gradient in percent

The Eq 12 is obtained by SLEMSA (Elwell, 1978).

$$LS (X) = (1 (0.76 + 0.53 s + 0.0765 s^2) / 25.65) \quad (\text{Eq. 2}).$$

The Eq. 13 used in this study was presented by Moore and Wilson (1992).

$$LS = [A/ 22.13] m [\sin\beta / 0.0896] n \quad (\text{Eq. 13})$$

Where:

A = upslope contributing area divided by the width of the contour that area contributes. The m and n = constants are equal to 0.6 and 1.3 , respectively.

β = land surface slope in degrees.



Figure 8) Slope length generated as “A” index.

In other words, A is the up-slope contributing area per unit width of cell spacing from which the water flows into a given grid cell.

Therefore, LS factor calculates the coefficients of the slope length, i.e. A , and the steepness, i.e. $\sin\beta$. For estimating $\sin\beta$ the slope layer should be generated by using DEM 50m. Figure 7 shows slope layer from less than 5° to greater than 99° slope.

To calculate A index based on command the flow accumulation values need to be calculated as slope length.

The equation 14 is used to calculate complete flow water on each of cells as a slope length. The slope length is shown in the Figure 8.



Figure 9) LS provided from DEM 50m by 50m.

$$\text{pow}([\text{flowacc50}] * 50 \text{ size} / 22.13, 0.4) * \text{pow}(\text{Sin}([\text{slope50}] / 0.0896, 1.3)) \quad (\text{Eq. 14})$$

In Eq. 14, LS factor could be generated with different cell size using the equation and it can be used as a factor in the topography factor.

Figures 10 show LS factor provided from DEM 50 by 50 meters. The process of generating LS factor is shown in Figure 11.

The last step in the suitability model is to combine the reclassified outputs, e.g. LS, C, K, R, and P, and to take those objectives which have more importance in the suitability model, the datasets that can be weighted, giving those datasets that should have more importance in the model a higher percentage influence

(weight) than the others into account. Continuous (floating-point) rasters must be reclassified as integer before they are used. Figure 11 shows establish a model builder using RUSLE.

4- Results and Analysis

The most popular model is advanced geostatistical procedure (kriging) generates an estimated surface from a scattered set of points with Z-values. Because Universal kriging assumes that spatial variation in Z-values has a drift or a trend in addition to the spatial correlation between the sample points, in this study, the Universal kriging Interpolation is used by second-order (quadratic surface) polynomial.

Typically, universal kriging incorporates a first-order (plane surface) or a second-order (quadratic surface) polynomial in the kriging process. This can be modeled by a deterministic, polynomial function. This polynomial is subtracted from the original measured points. Figure 12 shows the spherical mathematical model.

The semivariogram modeling is a key role between spatial description and spatial prediction. The main aim of using kriging is the prediction of attribute values at unknown locations. The empirical semivariogram prepares information on the spatial autocorrelation of datasets.

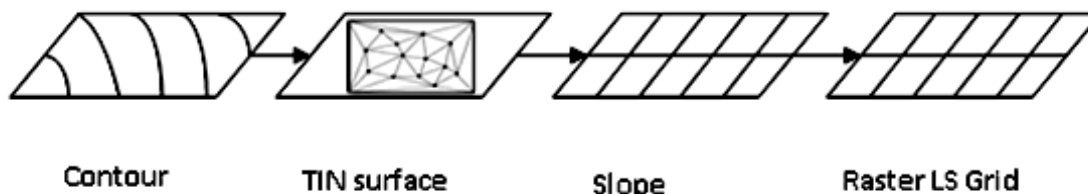


Figure 10) The process of generating LS factor.

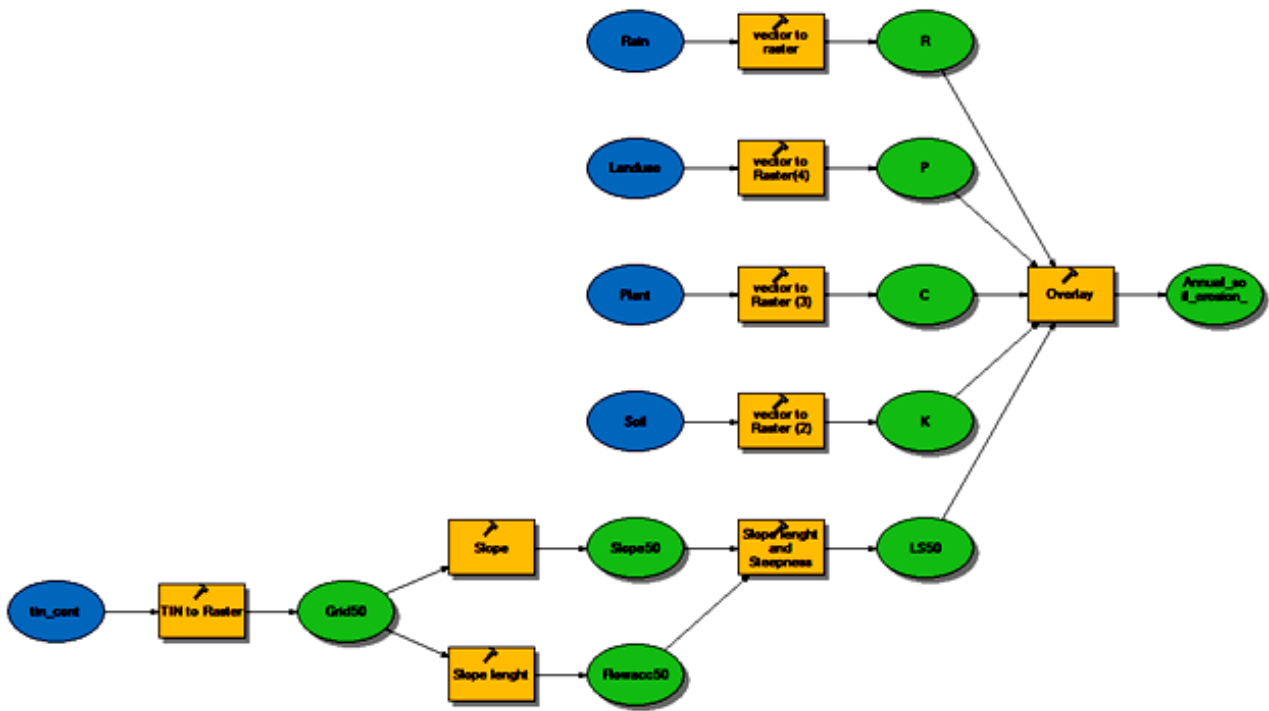


Figure 11) Model-builder designed for RUSLE.

Exploratory Spatial Data Analysis (ESDA) environment can be manipulated and explored based on different insights into the data, such as the distribution of the data, spatial autocorrelation, and covariation among multiple data sets. ESDA makes it possible to understand more about the phenomena so that better decisions about the related issues to the data can be made.

Randomly, 200 points selected for all DEMs sizes. The data distribution is roughly symmetrical and it is close to a normal distribution. The right tail indicates a relatively small number of samples with high elevation value concentrations. The distribution of the elevation attribute is shown by a histogram using the range of values classified into 10 classes and also the data is unimodal and fairly symmetric.

The kurtosis and skewness are two important factors in Table 4 Both coefficients show the distribution and symmetry of sample points that are identified as followed:

- Skewness coefficient for symmetrical distribution is equal to 0. If asymmetrical is toward the larger data, in this case the coefficient is positive and it is the negative if the coefficient is toward smaller ones.
- Kurtosis coefficient for normal distribution is equal 3. If the kurtosis is bigger than 3, it is leptokurtic but for smaller than 3, it will be platykurtic.

Skewness and kurtosis for data DEMs with 30, 50, 100, and 300 are shown in Table 4. The sample distributions of other produced DEMs have a relatively good symmetry.

SPHERICAL

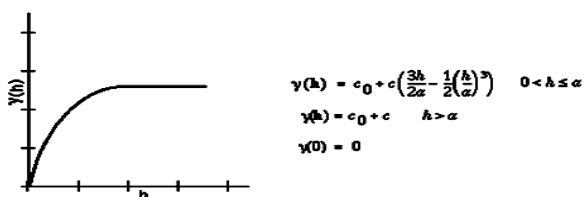


Figure 12) The spherical mathematical model

Table 4) The sample points distribution of DEMs after and before transformation using log method.

Cell Size (m)	Before transform				After transformation			
	Skewness	Kurtosis	mead	median	Skewness	Kurtosis	mead	median
DEM30	0.57288	2.668	954.51	880	-0.32772	4.3762	6.8212	6.7799
DEM50	0.59573	2.6684	971.55	896.55	-0.401	5.4134	6.8411	6.7986
DEM100	0.92768	2.0128	935.35	882.07	0.48715	2.363	6.8056	6.7823
DEM300	0.84979	2.837	902.97	902.97	0.42361	2.2999	6.8399	6.8057

4.1- The Semivariogram – Covariance Cloud Analysis

Using the semivariogram and covariance cloud can examine the spatial autocorrelation between the measured sample points. In the spatial autocorrelation it is assumed that those which are closer to one another are more alike. To do this, a semivariogram value which is the difference squared between the values of each pair of locations is drawn on the y-axis relative to the distance separating each pair on the x-axis. Each red point in the semivariogram/covariance cloud shows a pair of locations. In the semivariogram the close locations (far left on the x-axis) should have small semivariogram values (low on the y-axis) because the locations that are close to each other should be more alike. So the more the distance pairs of locations increases (move right on the x-axis), the more the semivariogram values increase (move up on the y-axis). However, when the cloud flattens out, it reaches a certain distance which indicates that the relationship between the pairs of locations beyond this distance is no longer correlated. Figure 13 to

Figure 16 show the semivariogram with 0, 45, 90, 135 degree direction.

According to Figure 13 to Figure 16, if semivariograms show that those location points are close together (near 0 on the x-axis) and have a higher semivariogram value (high on the y-axis) than would expect, these pair points should be investigated that each of them has a possibility to have inaccurate location.

Another factor is essential to interpret a semivariogram is direction. Semivariogram can also be examined by direction. A semivariogram plots the average semivariance against the directional component. One or more average semivariances may plot at the same distance. If spatial dependence exists among the sample points, then pairs of points that are closer in distance will have more similar values than pairs that are father apart (If spatial dependence has directional differences, then the semivariance values may change more rapidly in one direction than the other ones). In other words, the semivariance is expected to increase as the distance increases in the presence of spatial dependence.

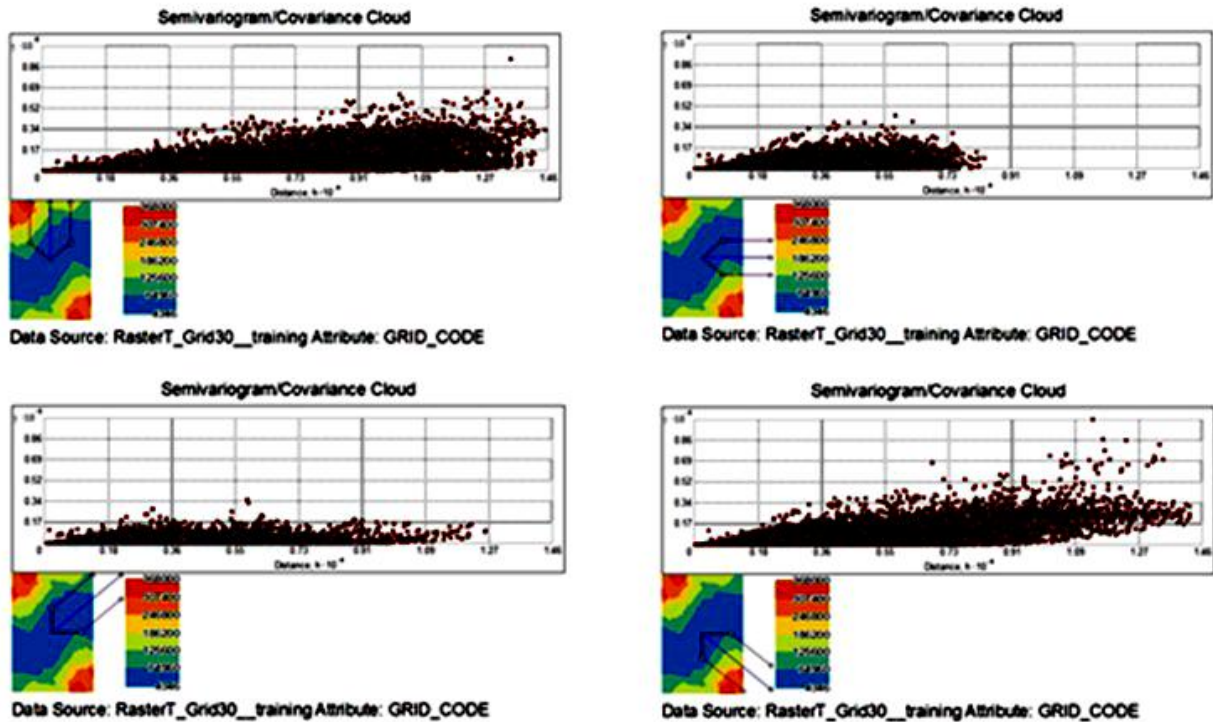


Figure 13) The semivariogram with 0°, 45°, 90°, and 135° directions (DEM 30m by 30m).

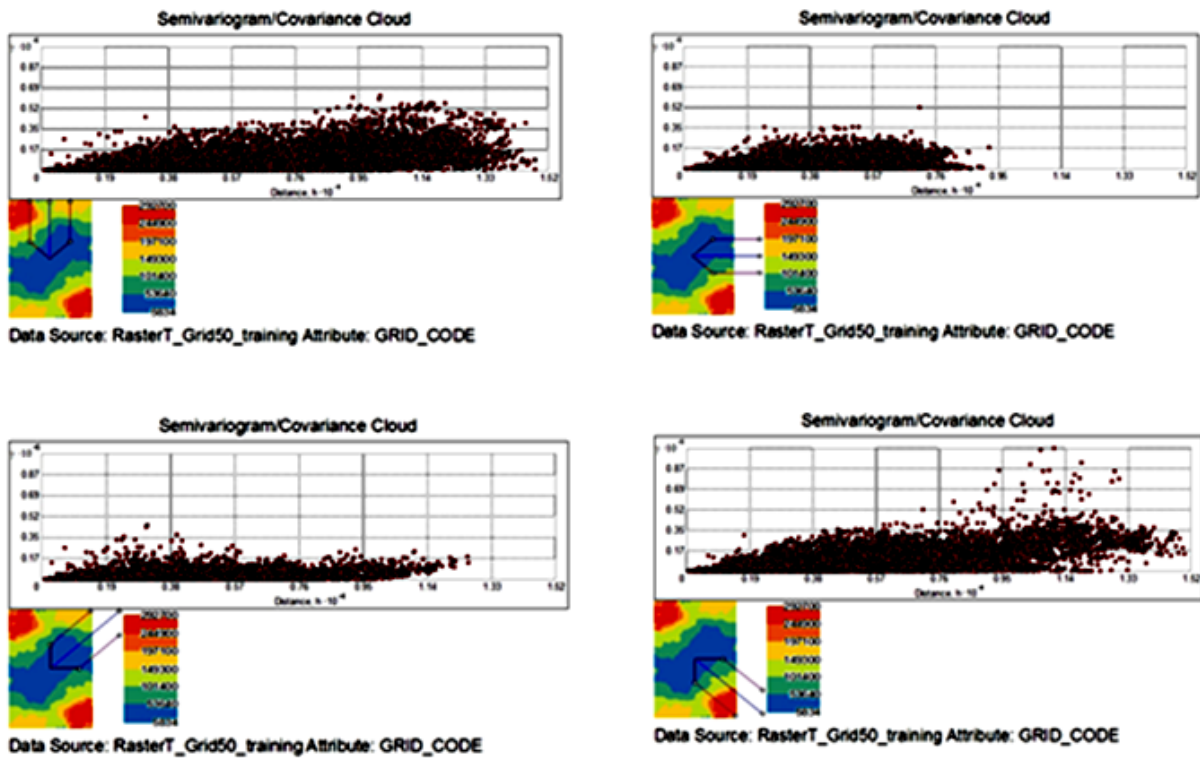


Figure 14) The semivariogram with 0°, 45°, 90°, and 135° directions (DEM 50m by 50m).

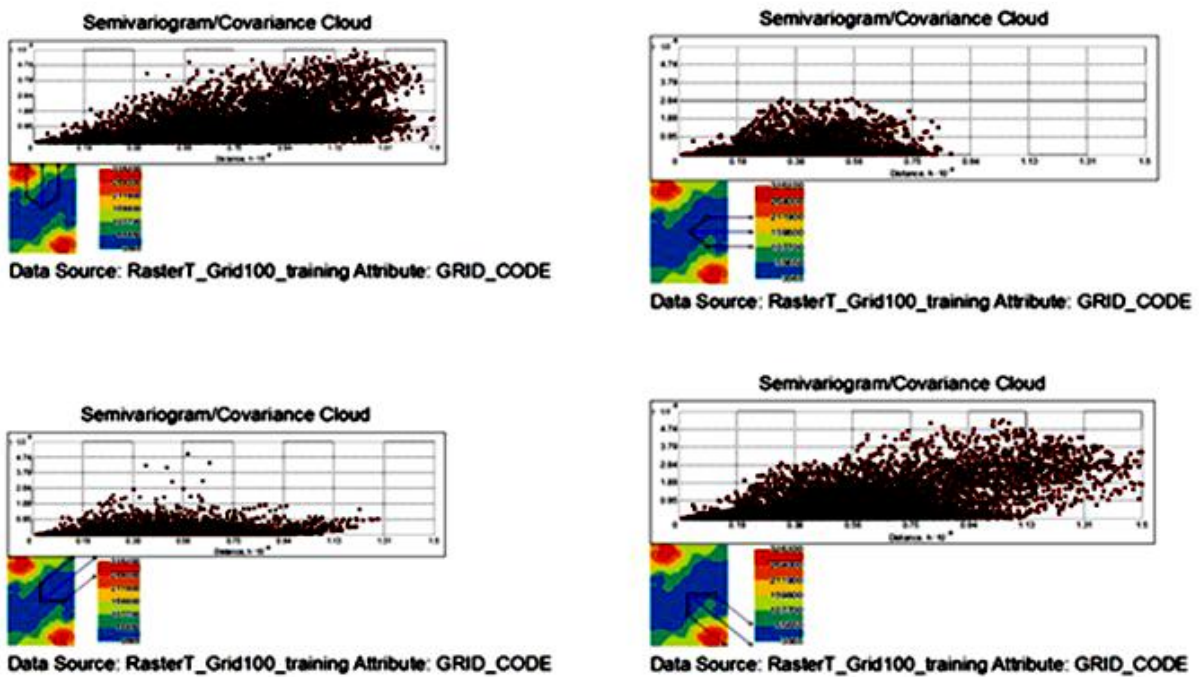


Figure 15) The semivariogram with 0°, 45°, 90°, and 135° directions (DEM 100m by 100m).

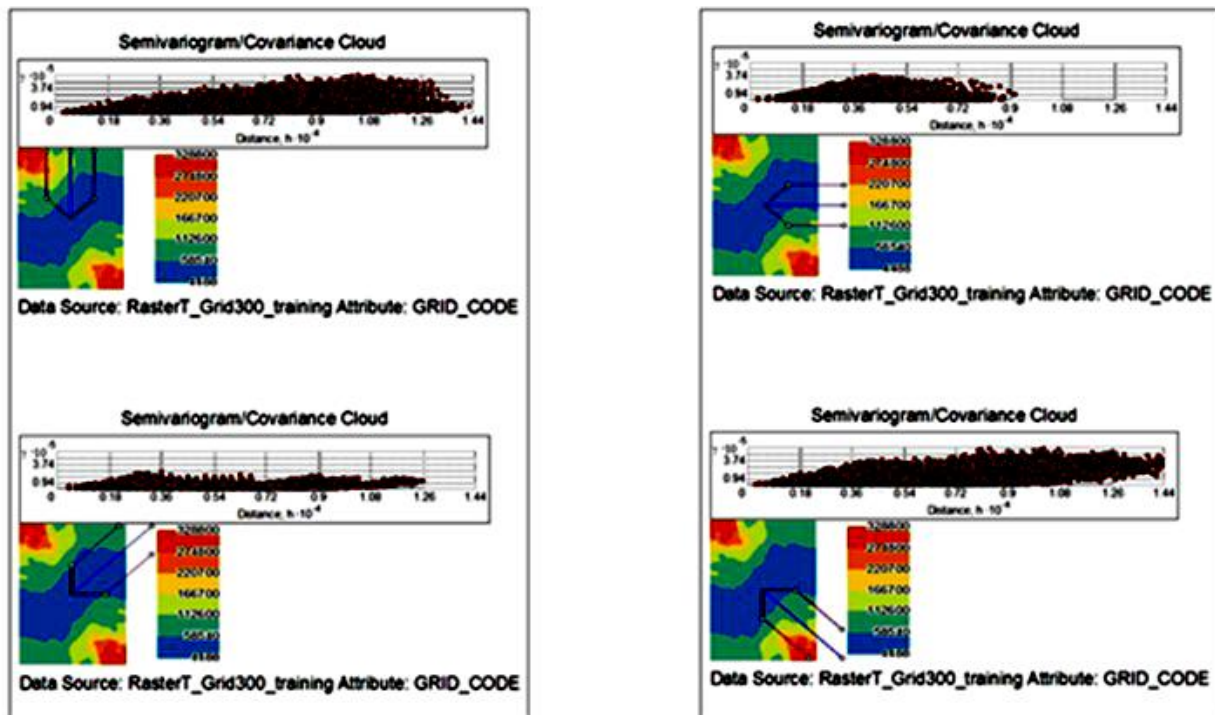


Figure 16) The semivariogram with 0°, 45°, 90°, and 135° directions (DEM 300m by 300m).

4.2- Implementation of model

In order to provide an efficient and optimal model, it requires to investigating the obtained exact statistical data. Figure 17 shows the points scattered in the empirical semivariogram. The geostatistical analyst calculates some default parameters for models such as nugget, partial sill, lag, etc. The lag is the size of the distance classes in which pairs of locations are grouped.

The grouping of the data values in this way is called “binning”. Because the data has been binned, there are fewer points on the semivariogram graph. Therefore, the lag size should be adjusted. The lag size can be the average distance between neighboring DEMs samples that are obtained. The best lag size has determined in this study is 300 meters. Figure

17 shows how to fit the data and the obtained values for nugget and sill.

Decreasing variance in the nugget implies a reduction of noise and within-cell spatial variability due to the data resampling. One other important characteristic is the ratio of the nugget to the sill $[C_0 / (C_0 + C)]$ which reflects a quantity called spatial variance. This ratio for DEM 30m is 0.512693 and its value for DEMs

50m increases to 0.965852. When the amount of DEMs cell sizes increases the nugget values decreases in return. As results, DEM 50-meter cell size leads to maximum nugget and spatial variance. Therefore, this research shows that DEM 50m is the most suitable for topographic map with 20 meter interval which gives the maximum information for calculating the LS factor.

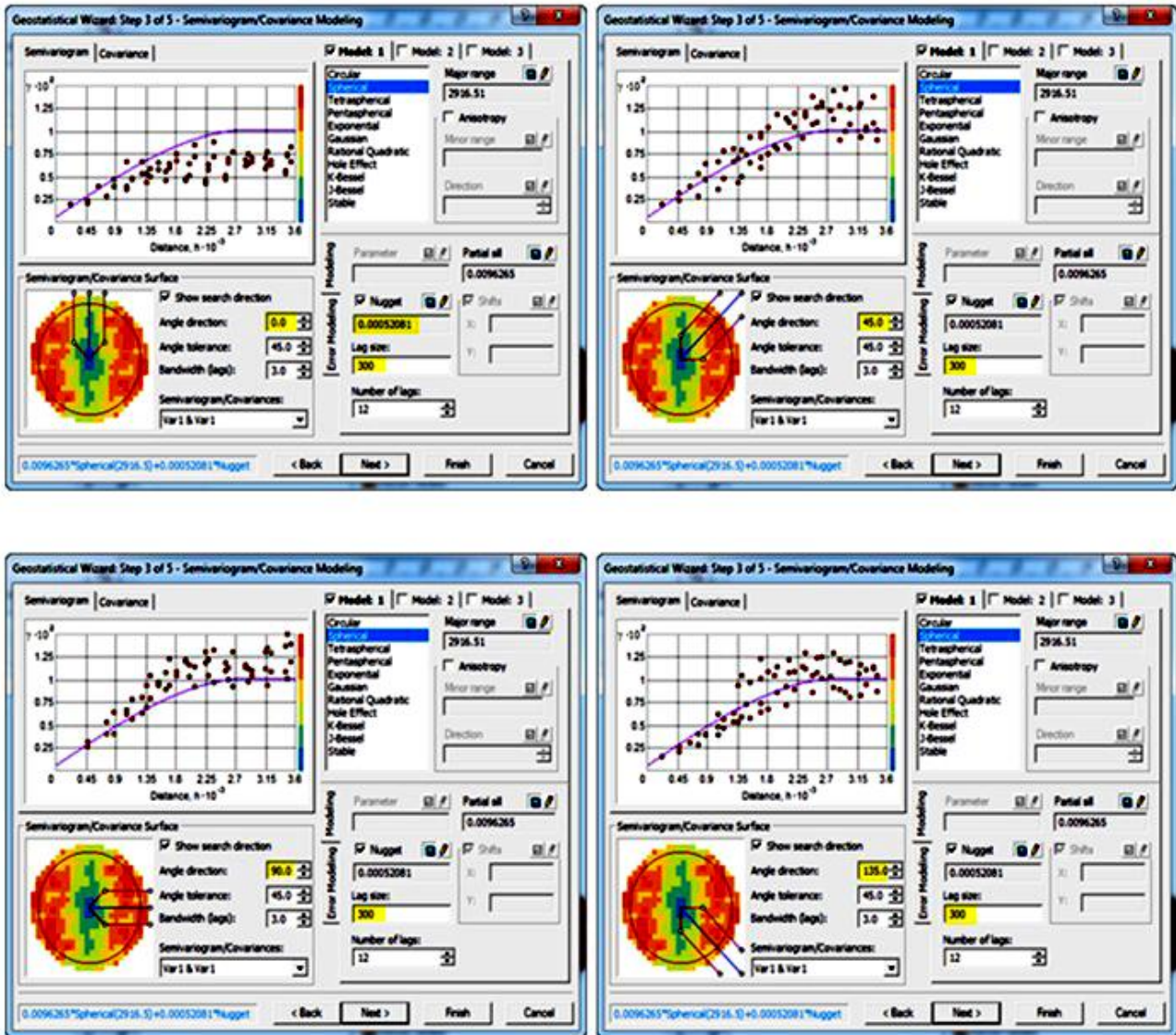


Figure 17) The semivariogram fitted for DEM 300m by 300m.

Figure 18 shows the map plotted for DEMs based on 50m cell size using universal kriging method. As it can be seen on this map, the distribution DEMs maximum values in the Southeast have greater height than north and northwest.

Finally, via choosing the most appropriate cell size the annual soil erosion and the rest of created factors can be calculated using RUSLE equation. Figure 19 shows the areas that were affected by erosion and annual soil erosion maps. The dots of red colored in the figure have more potential ability for soil erodibility.

According to the results, by using geostatistical techniques which can identify the best DEM cell size in order to make the suitable raster analysis for decision in the case of DEM spacing.

Basically, these techniques lead to find DEMs 50m from topographic map with 20m interval contour lines.

Table 5) The data captured from the semivariogram.

Grid sell size (m)	Model	Nugget C0	Partial Sill C1	Sill $C = C_0 + C_1$	ME	RMS	C1/C
DEM30	Spherical	0.0075609	0.0079548	0.0155157	0.02952	0.2708	0.512693
DEM50	Spherical	0.0053492	0.01513	0.1566492	0.03321	0.2435	0.965852
DEM100	Spherical	0.0009848	0.0082398	0.0092246	-0.00075	0.2671	0.893240
DEM300	Spherical	0.0005208	0.0096265	0.0101473	-0.00306	0.1594	0.948675

Universal Kriging 30m Map

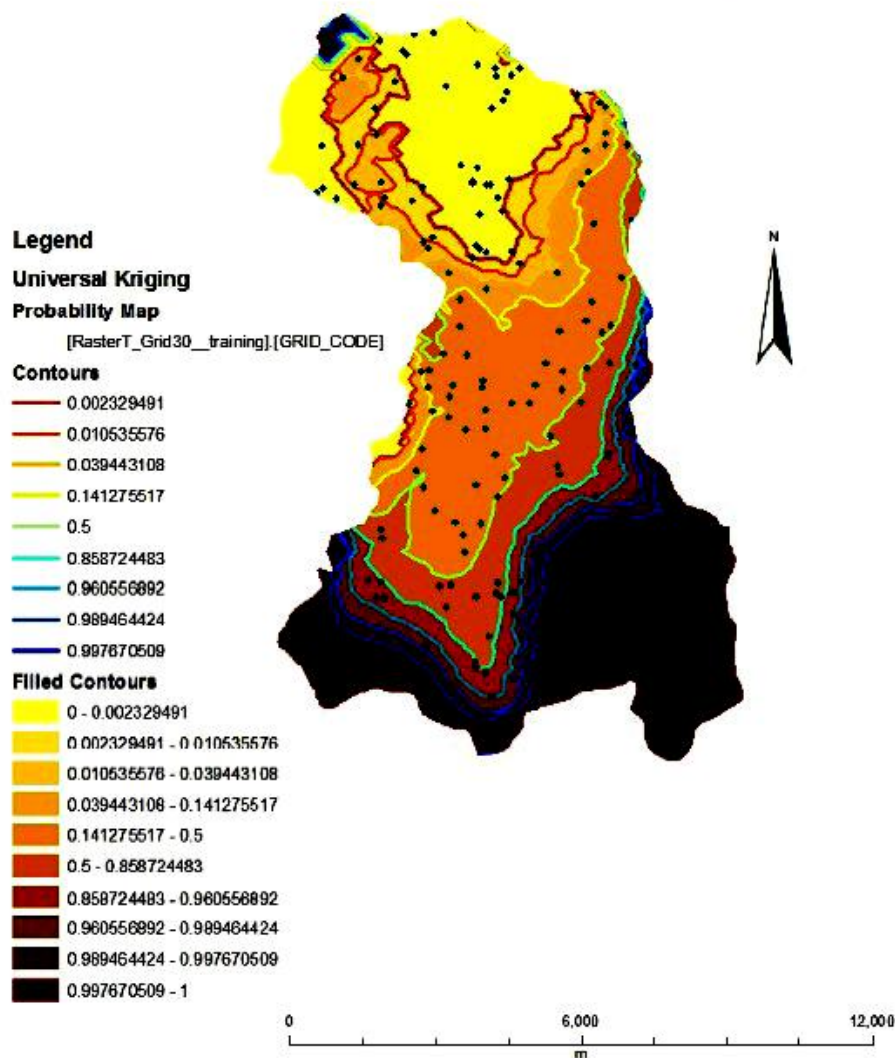


Figure 18) Universal Kriging map with DEM 50m.

Annual Soil Erosion Map

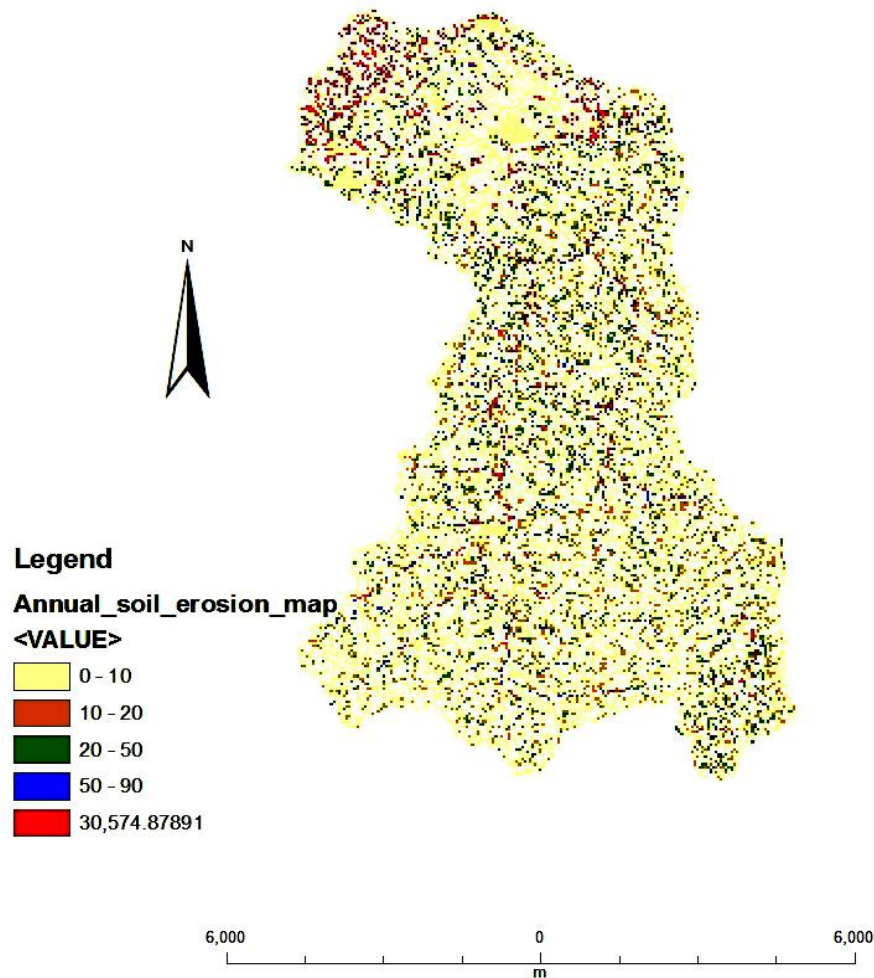


Figure 19) Annual soil erosion map.

5- Conclusions

Modeling soil erosion due to the complexity of the earth and using GIS requires several essentially factors such as the best cell size, high resolution DEM (digital elevation model), formulation of erosion models suitable for digital representation of spatially parameters distributed, and reliable computation for estimation topographic parameters. The geostatistical analyst tool and its toolset like kriging in GIS and also its other details, e.g. the digitized contour lines which are taken from topographic map are very useful for the accurate calculations of the appropriate DEMs.

In general, this study not only demonstrates that increases in cell sizes of DEMs which can cause losing some of information and can reduce the accuracy and quality of the results in such researches but also shows the important role of the geostatistical analysis techniques in this case.

The estimated RUSLE erosion and specific erosion values illustrate relatively high variability in terms of spatial and temporal characteristics together with the effect of using different grid cell size. The RUSLE model is able to calculate annual soil erosion in the long time by using several parameters, e.g. slope length, steepness, Support practice, soil erodibility, and rainfall. This method is one of the most important ways for calculating the LS

or topographic factor, because the accuracy and quality of the obtained results depends on resolution of DEM. This study deals with geostatistical methods and interpolation for how to use and carry out kriging method in the researches. The plotted results from semivariograms show that for preparation of the digital elevation model with best spatial dependency, the DEM 50m provided from topographic map with 20m interval contour lines is the best option.

In general, the results of this study have confirmed that the geostatistical analysis and statistical approaches together can be applied to select adequate cell spacing in DEM and also to predict topographical factor in RUSLE model.

References

- Anima, S., Tirkey, P., Nathawat, S. 2013. Use of satellite data, GIS and RUSLE for estimation of average annual soil loss in Daltonganj watershed of Jharkhand (India). *Journal of Remote Sensing Technology*: 1, 20–30.
- Blanco, H., Lal, R. 2008. *Principles of soil conservation and management*, Heidelberg, Germany. Springer.
- Chang, T. 2010. *Introduction to Geographic Information Systems*, (5th edition). New York, USA. McGraw- Hill.
- FAO. 2016. *Status of the World's Soil Resources*.
- Gelagay, S. 2016. RUSLE and SDR Model Based Sediment Yield Assessment in a GIS and Remote Sensing Environment, A Case Study of Koga Watershed, Upper Blue Nile Basin, Ethiopia. *Hydrology: Current Research*: 7, 239–248.
- Jim Ritter, P. Eng. 2015. *Replaces OMAFRA Factsheet, Soil Erosion – Causes and Effects*, Order No. 87–040.
- Kayet, N., Chakrabarty, A. 2016. Hyper spectral Image processing for Forest types Mapping and forest health monitoring, a case study in the buffer zones of iron mining belts of Saranda forest, Jharkhand, India.
- Kayet, N., Pathak, Kh., Chakrabarty, A., Sahoo, S. 2018. Evaluation of soil loss estimation using the RUSLE model and SCS-CN method in hill slope mining areas. *Journal of International Soil and Water Conservation Research*: 6, 31–42.
- Oshaksaraie, L., Noor E. A., Azuraliza, A. B., Khairul, N. A. 2009. An Expert System Prototype for Minimizing Soil Erosion on Construction Site in Malaysia. *European Journal of Scientific Research*: 33, 454–460.
- Merritt, W. S., Letcher, R. A., Jakeman, A. J. 2003. Are view of erosion and sediment transport models. *Journal of Environmental Modelling and Software*: 18, 761–799.
- Moore, I. D., Wilson, J. P. 1992. Length-slope factors for the Revised Universal Soil Loss Equation, simplified method or estimation. *Journal of Soil Water Conservation*: 45, 423–428.
- Morgan, R. C. 1986. *Soil Erosion and Conservation*. Journal of Longman Scientific and Technical UK.
- Moses, A. N. 2017. GIS-RUSLE Interphase Modelling of Soil Erosion Hazard and Estimation of Sediment Yield for River Nzoia Basin in Kenya. *Journal of Remote Sensing and GIS*: 6, 205–217.
- Renard, K. G., Ferreira, V. A. 1993. RUSLE model description and database sensitivity. *Journal of Environmental Quality*: 22, 458–466.
- Renard, K. G., Freimund, J. R. A. 1994. Using Monthly Precipitation Data to Estimate the R factor in the Revised USLE. *Journal of Hydrology*: 157, 287–306.
- Renard, K. G., Foster, G. R., Weesies, G. A., McCool, D. K. 1997. *Predicting soil erosion by water, a guide to conservation planning*

- with the Revised Universal Soil Loss Equation (RUSLE), Agric. Handb, US Department of Agriculture, Washington, DC, V. 703.
- Sahoo, S., Dhar, A., Kayet, N., Kar, A. 2016. Detecting water stress scenario by land use/land cover changes in an agricultural command area. *Journal of Spatial Information Research*: 1–11.
- Soil and Water Conservation Society. 1993. RUSLE user's guide. Soil and Water Cons. Soc. Ankeny, IA. 164.
- Tung G. P., Degener, J., Kappas, M. 2018. Integrated universal soil loss equation (usle) and geographical information system (gis) for soil erosion estimation in a sap basin, central Vietnam. *Journal of International Soil and Water Conservation Research*: <https://doi.org/10.1016/j.iswcr.2018.01.001>.
- Turner, B. L., Fuhrer, J., Wuellner, M., Menendez, H. 2018. Scientific case studies in land-use driven soil erosion in the central United States, Why soil potential and risk concepts should be included in the principles of soil health. *Journal of International Soil and Water Conservation Research*. <https://doi.org/10.1016/j.iswcr.2017.12.004i>.
- Wang, G., Gartner, P., Parysow, A. B., Anderson. 2000. Spatial prediction and uncertainty analysis of topographical factors for the Revised Universal Soil Loss Equation. *Journal of Soil and Water Conservation*: 55, 373–382.
- Wang, G., Gartner, P., Parysow, A. B., Anderson. 2001. Spatial prediction and uncertainty assessment of topographic factor for the Revised Universal Soil Loss Equation using digital elevation models. *Journal of Photogrammetry and Remote Sensing*: 56, 65–80.
- Webster, R., Oliver, M. A. 2011. *Geostatistics for environmental science*. John Wiley and Sons, LTD. Toronto, Canada, 271.
- Wischmeier, W. H., Smith. D. 1978. Predicting rainfall-erosion losses - a guide to conservation planning. AH-537. U.S. Dept. Agr., Washington, D.C.
- www.omafra.gov.on.ca/english/engineer/facts/12-053.htm Jan 4, 2016.